The HKU Scholars Hub    The University of Hong Kong    香港大學學術庫

| | |
|---|---|
| **Title** | **Predissociation linewidths of the (1,0)-(12,0) Schumann-Runge absorption bands of O2 in the wavelength region 179-202 nm** |
| **Author(s)** | **Cheung, ASC; Yoshino, K; Esmond, JR; Chiu, SSL; Freeman, DE; Parkinson, WH** |
| **Citation** | **The Journal Of Chemical Physics, 1990, v. 92 n. 2, p. 842-849** |
| **Issued Date** | **1990** |
| **URL** | **http://hdl.handle.net/10722/147697** |
| **Rights** | **Creative Commons: Attribution 3.0 Hong Kong License** |

# Predissociation linewidths of the (1,0)–(12,0) Schumann–Runge absorption bands of O₂ in the wavelength region 179–202 nm

A. S.-C. Cheung,[a] K. Yoshino, J. R. Esmond, S. S.-L. Chiu,[a] D. E. Freeman, and W. H. Parkinson

*Harvard-Smithsonian Center for Astrophysics, Cambridge, Massachusetts 02138*

A nonlinear least-squares method of retrieving predissociation linewidths from the experimental absolute absorption cross sections of Yoshino *et al.* [Planet. Space Sci. **31**, 339 (1983)] has been applied to the (1,0)–(12,0) Schumann–Runge bands of oxygen. Predissociation linewidths deduced for the Schumann–Runge bands are larger than the theoretical predictions of Julienne [J. Mol. Spectrosc. **63**, 60 (1976)] and the latest measurements of Lewis *et al.* [J. Quant. Spectrosc. Radiat. Transfer **36**, 187 (1986)]. The larger linewidths found will have an impact on calculations of solar flux penetration into the Earth's atmosphere and of the photodissociation rates of trace species in the upper atmosphere. Systematic variation of predissociation linewidths with rotational quantum number is observed in the bands ($v'$,0) with $v' = 6, 8, 9, 11,$ and 12.

## I. INTRODUCTION

The predissociation of the oxygen molecule in the Schumann–Runge bands is of particular importance in atmospheric chemistry. The Schumann–Runge absorption bands, which extend from 175 to 205 nm, are extensively predissociated, so that the absorption cross section is essentially the cross section for the production of $O(^3P)$ atoms. This cross section consists of hundreds of broadened and often overlapping rovibronic lines, and the predissociation of $^{16}O_2$ is the main source of odd oxygen in the atmosphere above 60 km. In addition, the cross section may vary by two orders of magnitude between peaks and valleys of a given vibronic band, so that details of the rovibronic linewidths determine the depth to which solar radiation may penetrate into the atmosphere, where it is available to photodissociate important trace species.[1–3]

The determination of linewidths and oscillator strengths from measured absorption cross sections, though simple in principle, is straightforward only if the instrumental bandwidth of the spectrometer is small compared with the width of the absorption feature being measured.[4] For the Schumann–Runge bands of $O_2$, the only absolute cross sections published, apart from the measurements of Ackerman *et al.*[5] at several atomic line wavelengths, are our measurements throughout the region 179.5–201.5 nm of the (1, 0)–(12, 0) bands[6,7] and our measurements throughout the region 195–205 nm[8]; all of our measurements were performed with a 6.65 m scanning spectrometer.[9]

The predissociation is caused by four repulsive states, namely, $^1\Pi_u$, $^3\Pi_u$, $^5\Pi_u$, and $^3\Sigma_u^+$, which cross the upper $B\,^3\Sigma_u^-$ state of the Schumann–Runge system in its bound region.[10] The theoretical investigations of Julienne and Krauss,[11] and Julienne[12] have shown that both the level shifts and linewidths can be attributed to perturbations dominated by the $^5\Pi_u$ state, with other states playing minor roles in the predissociation. Nevertheless, accurate predissociation linewidth measurements for the various vibrational levels are required to provide a meaningful comparison of different sets of linewidths calculated from theoretical parameters.

## II. PROCEDURE

The numerical techniques applied here have been described elsewhere.[13–15] Linewidths as parameters are determined through a nonlinear least-squares procedure that iterates between the observed cross section and a synthetic spectrum corresponding to the experimental conditions. An absorption line profile observed by a particular spectrometer under ordinary conditions is the convolution of the true line profile with the instrumental function, but if the width of the spectral feature is larger than the instrumental bandwidth, true absorption cross sections can be obtained. The rovibronic levels of the upper state of the Schumann–Runge bands of $O_2$ are predissociated by various repulsive states and the widths of the overlapping lines exceed our instrumental bandwidth, so that true absorption profiles are obtained for the (1, 0)–(12, 0) bands.[6,7]

The absorption cross section $\sigma(v)$ is related to absorption intensity by the formula

$$\ln[I_0(v)/I(v)] = N\sigma(v) \qquad (1)$$

in which $I_0(v)/I(v)$ is the ratio of the incident intensity $I_0(v)$ to the intensity $I(v)$ transmitted through a medium of column density $N(\mathrm{cm}^{-2})$. The absorption cross sections fitted in this study throughout the region 179–202 nm are those of the (1,0)–(12,0) bands.[6–8] All of the measurements were performed with a 6.65 m scanning photoelectric spectrometer having an instrumental width [full width at half-maximum (FWHM)] of 0.0013 nm ($\simeq 0.4\ \mathrm{cm}^{-1}$).

To calculate synthetic spectra of the cross section, we need knowledge of or assumptions about the line center positions, line strengths, and line profiles. These items are discussed below.

---

[a] International Exchange Scholar, Smithsonian Institution, 1987-1988. Present address: Chemistry Department, University of Hong Kong, Hong Kong.

## A. Line center positions

The $B$–$X$ transition frequencies have been calculated by using the $^3\Sigma$ state Hamiltonian and the molecular spectroscopic constants tabulated in Cheung *et al.*[16] Because of large predissociation linewidths and relatively small triplet splittings, the experimental spectrum exhibits only partially resolved or unresolved triplet structures in the (1,0)–(12,0) bands.[6] In this study, the triplets arising from the transitions between fine structure components $F_1(N)$, $F_2(N)$, and $F_3(N)$ of the lower and the upper states are treated as groups, in the sense that their relative line centers and relative line strengths (see the next section) are held fixed. For example, the $R(N)$ composite line consists of $R_1(N)$, $R_2(N)$, and $R_3(N)$ component lines with different $J$ values; these three lines are treated as a group in the fit. This treatment introduces a desirably restrictive contraint because, in a least-squares fit of an unresolved spectral envelope, there are generally multiple solutions of which only one is physically relevant.

## B. Line strengths

An individual line strength involves a product of a Hönl–London factor and a Boltzmann population factor. The Hönl–London factors for a $^3\Sigma_u^- - ^3\Sigma_g^-$ transition given by Tatum and Watson[17] for the intermediate Hund case are used in this work, together with the Boltzmann population factors calculated in the usual way. The partially resolved or unresolved fine structure components of a line have been treated as a group with constant line strength ratio during the fitting procedure.

## C. Line profiles

The broadening of a rotational line due to thermal molecular motion (Doppler line shape) and predissociation (Lorentzian line shape) should be described by the resultant Voigt profile. However, if the predisociation linewidth is considerably larger than the Doppler linewidth, the simpler Lorentzian profile suffices to describe the line shape.[18] The Doppler linewidth (FWHM) of oxygen at room temperature near 50,000 cm$^{-1}$ is about 0.12 cm$^{-1}$, whereas the predissociation linewidths are in the range 0.8–4.0 cm$^{-1}$ for the bands $(v',0)$ where $v' = 1$–12 so that Lorentzian profiles may justifiably be used in our analysis (see also Sec. III).

The spectral features in intervals of 30–70 cm$^{-1}$ are fitted simultaneously. In the least-squares fitting of the calculated to the observed absorption cross section, the only parameters varied are the predissociation linewidth of a group of fine structure components and the absolute line intensity of the group. Within a group of fine structure components, the predissociation linewidths are assumed to be equal and, as already mentioned, the relative line strengths are determined by the known Hönl–London and Boltzmann factors. The line center positions of the fine structure components are generated from our spectroscopic constants.[16] In the bandhead region, satellite and forbidden branches occur, in addition to the main $P$ and $R$ branches, and are incorporated in the synthetic cross section. Except for the $P(1)$ line which consists of a single component $P_1(1)$, the main branches
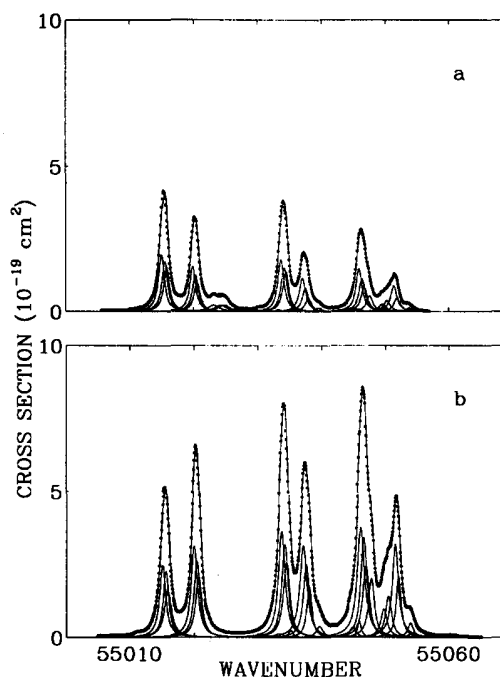


FIG. 1. Absorption cross section near the bandhead of the (10,0) Schumann–Runge band of $O_2$ at (a) 295 K (top) and (b) 79 K (bottom). In each diagram, the uppermost curve is synthesized from the lower fine structure component (Lorentzian) curves to fit the measured cross sections, represented by dots.

exhibit the usual triplet structure and consist of components $P_i$ and $R_i$ ($i = 1$–3). Figures 1(a) and 1(b) show the synthetic and experimental absorption cross sections for the bandhead region of the (10,0) band at 295 and 79 K, respectively. The discrete points are the experimental cross sections to which the uppermost curve is fitted by the least-squares procedure discussed above. The agreement between the synthetic and experimental cross sections is excellent at both temperatures. The lower curves are the Lorentzian components, the sum of which yields the uppermost resultant synthetic cross section. Weak lines around 55 023 cm$^{-1}$ on Fig. 1(a) are $P(21)$ of the (11,0) band which are not seen in Fig. 1(b) because of the lower temperature.

## III. RESULTS AND DISCUSSION

Table I lists 395 predissociation linewidths (FWHM) deduced from the absorption cross sections of the (1,0)–(12,0) bands. Both 295 and 79K absorption cross sections were analyzed separately for bands $(v',0)$ with $v' = 3$–12; for $v' = 1$ and 2, only the 295K cross sections were fitted. In Table I, linewidths are given for $P$ and $R$ branch lines and $N'$ is the upper state rotational quantum number, so that both lines of the same $N'$ level can readily be compared. The results of such a fitting procedure are not overly sensitive to the change of the linewidth, with the result that the scatter is fairly large.

In Table II, where our predissociation linewidths are compared with others, our values are averages, for each band, of all the linewidths listed for that band in Table I; the uncertainties in our mean values are $1\sigma$ limits. Our average

TABLE I. Predissociation linewidths ($cm^{-1}$) of the Schumann–Runge bands of $O_2$.[a]

| | (1,0) Band $\Gamma_0 = 1.07(5)$ $10^3\alpha = -1.02(25)$ 295 K | | (2,0) Band $\Gamma_0 = 0.70(1)$ $10^3\alpha = +0.15(7)$ 295 K | |
|---|---|---|---|---|
| $N'$ | $P$ | $R$ | $P$ | $R$ |
| 0 | 1.02 | | 0.74 | |
| 2 | 1.31 | 0.82 | 0.70 | 0.74 |
| 4 | 1.21 | 0.93 | 0.70 | 0.70 |
| 6 | 0.98 | 1.01 | 0.65 | 0.67 |
| 8 | 0.90 | 1.06 | 0.68 | 0.67 |
| 10 | 0.90 | 1.08 | 0.71 | 0.77 |
| 12 | 0.79 | 1.09 | 0.69 | 0.72 |
| 14 | 0.76 | 1.01 | 0.70 | 0.76 |
| 16 | 0.69 | 0.76 | 0.76 | 0.78 |
| 18 | | 0.75 | 0.73 | 0.73 |
| 20 | | 0.64 | | |

| | (3,0) Band $\Gamma_0 = 1.74(3)$ 295 K | | $10^3\alpha = +0.34(14)$ 79 K | | (4,0) Band $\Gamma_0 = 3.87(7)$ 295 K | | $10^3\alpha = +0.00(43)$ 79 K | |
|---|---|---|---|---|---|---|---|---|
| $N'$ | $P$ | $R$ | $P$ | $R$ | $P$ | $R$ | $P$ | $R$ |
| 0 | 1.47 | | 1.83 | | 4.21 | | 4.37 | |
| 2 | 1.72 | 1.47 | 1.75 | 1.83 | 3.66 | 4.21 | 3.67 | 4.37 |
| 4 | 1.76 | 1.78 | 1.71 | 1.85 | 3.62 | 4.21 | 3.89 | 4.37 |
| 6 | 1.75 | 1.65 | 1.77 | 1.67 | 3.72 | 3.66 | 3.45 | 3.67 |
| 8 | 1.83 | 1.92 | 1.79 | 1.76 | 3.67 | 3.62 | 3.77 | 3.89 |
| 10 | 1.73 | 1.89 | 1.73 | 1.82 | 3.84 | 3.72 | 3.93 | 3.45 |
| 12 | 1.73 | 1.94 | | 1.90 | 4.03 | 3.67 | | 3.77 |
| 14 | 1.78 | 1.94 | | | 3.72 | 3.77 | | 3.93 |
| 16 | 1.79 | 1.88 | | | 3.95 | 3.91 | | |
| 18 | 1.98 | 1.72 | | | 3.96 | 3.56 | | |
| 20 | | 1.92 | | | | 4.44 | | |
| 22 | | 1.83 | | | | | | |

| | (5,0) Band $\Gamma_0 = 2.14(2)$ 295 K | | $10^3\alpha = -0.14(11)$ 79 K | | (6,0) Band $\Gamma_0 = 1.59(2)$ 295 K | | $10^3\alpha = +1.27(8)$ 79 K | |
|---|---|---|---|---|---|---|---|---|
| $N'$ | $P$ | $R$ | $P$ | $R$ | $P$ | $R$ | $P$ | $R$ |
| 0 | 2.15 | | 2.22 | | 1.55 | | 1.58 | |
| 2 | 2.10 | 2.15 | 2.19 | 2.22 | 1.59 | 1.55 | 1.66 | 1.67 |
| 4 | 2.05 | 2.29 | 2.15 | 2.22 | 1.64 | 1.69 | 1.54 | 1.58 |
| 6 | 2.09 | 2.10 | 2.07 | 2.19 | 1.69 | 1.59 | 1.60 | 1.66 |
| 8 | 2.08 | 2.05 | 2.08 | 2.15 | 1.78 | 1.64 | 1.71 | 1.54 |
| 10 | 2.05 | 2.09 | 2.13 | 2.07 | 1.79 | 1.69 | 1.77 | 1.60 |
| 12 | 2.15 | 2.08 | 2.27 | 2.08 | 1.88 | 1.78 | 1.85 | 1.71 |
| 14 | 2.08 | 2.05 | | 2.13 | 1.93 | 1.79 | 1.98 | 1.77 |
| 16 | 2.07 | 2.15 | | 2.27 | 2.06 | 1.88 | | 1.85 |
| 18 | | 2.08 | | | 2.17 | 1.93 | | 1.98 |
| 20 | | 2.07 | | | 2.30 | 2.06 | | |
| 22 | | | | | | 2.17 | | |
| 24 | | | | | | 2.30 | | |

TABLE I. (*continued*).

| N' | (7,0) Band | | | | (8,0) Band | | | |
|---|---|---|---|---|---|---|---|---|
| | $\Gamma_0 = 2.01(2)$ 295 K | | $10^3\alpha = +0.03(11)$ 79 K | | $\Gamma_0 = 1.83(2)$ 295 K | | $10^3\alpha = +0.58(8)$ 79 K | |
| | P | R | P | R | P | R | P | R |
| 0 | 2.02 | | 1.98 | | 1.88 | | 1.79 | |
| 2 | 2.23 | 2.02 | 2.18 | 1.98 | 1.81 | 1.88 | 1.74 | 1.79 |
| 4 | 1.98 | 2.02 | 2.01 | 1.98 | 1.68 | 1.81 | 1.88 | 1.74 |
| 6 | 1.98 | 2.23 | 1.91 | 2.18 | 1.88 | 1.95 | 1.82 | 1.97 |
| 8 | 1.94 | 1.98 | 1.86 | 2.01 | 2.08 | 1.87 | 1.86 | 1.78 |
| 10 | 1.98 | 1.98 | 1.88 | 1.91 | 2.01 | 1.83 | 1.86 | 1.81 |
| 12 | 1.92 | 1.94 | | 1.86 | 1.95 | 1.87 | 1.89 | 1.80 |
| 14 | 2.19 | 1.98 | | 1.88 | 1.97 | 1.86 | 2.05 | 1.92 |
| 16 | 2.09 | 1.92 | | | 1.90 | 1.99 | | 2.04 |
| 18 | 2.01 | 2.19 | | | 2.15 | 2.20 | | 2.10 |
| 20 | 2.03 | 2.09 | | | 2.21 | 2.00 | | |
| 22 | | 2.01 | | | | 2.05 | | |
| 24 | | 2.03 | | | | 2.04 | | |

| N' | (9,0) Band | | | | (10,0) Band | | | |
|---|---|---|---|---|---|---|---|---|
| | $\Gamma_0 = 0.88(2)$ 295 K | | $10^3\alpha = +1.00(9)$ 79 K | | $\Gamma_0 = 1.13(2)$ 295 K | | $10^3\alpha = -0.26(10)$ 79 K | |
| | P | R | P | R | P | R | P | R |
| 0 | 0.95 | | 0.84 | | 1.12 | | 1.23 | |
| 2 | 0.84 | 0.90 | 0.80 | 0.79 | 1.14 | 1.19 | 1.14 | 1.09 |
| 4 | 0.99 | 0.95 | 0.91 | 0.84 | 1.11 | 1.12 | 1.15 | 1.23 |
| 6 | 0.96 | 0.92 | 0.91 | 0.92 | 1.19 | 1.13 | 1.09 | 1.19 |
| 8 | 0.98 | 0.95 | 0.88 | 0.91 | 1.09 | 0.99 | 1.08 | 1.16 |
| 10 | 0.99 | 1.01 | 0.98 | 0.97 | 1.10 | 0.97 | 0.99 | 1.08 |
| 12 | 1.06 | 1.03 | | 0.99 | 1.01 | 1.04 | | 1.01 |
| 14 | 1.03 | 1.02 | | 1.25 | 1.09 | 1.12 | | 0.99 |
| 16 | 1.13 | 1.12 | | | 1.06 | 1.01 | | |
| 18 | 1.28 | 1.37 | | | 0.93 | 1.17 | | |
| 20 | 1.44 | 1.17 | | | | 1.20 | | |
| 22 | | 1.24 | | | | 0.96 | | |

| N' | (11,0) Band | | | | (12,0) Band | | | |
|---|---|---|---|---|---|---|---|---|
| | $\Gamma_0 = 1.32(2)$ 295 K | | $10^3\alpha = +1.23(12)$ 79 K | | $\Gamma_0 = 0.76(2)$ 295 K | | $10^3\alpha = +1.07(11)$ 79 K | |
| | P | R | P | R | P | R | P | R |
| 0 | 1.40 | | 1.43 | | 0.70 | | 0.74 | |
| 2 | 1.30 | 1.14 | 1.15 | 1.23 | 0.72 | 0.71 | 0.76 | 0.83 |
| 4 | 1.42 | 1.40 | 1.37 | 1.43 | 0.64 | 0.80 | 0.80 | 0.89 |
| 6 | 1.47 | 1.49 | 1.35 | 1.55 | 0.85 | 0.89 | 0.78 | 0.90 |
| 8 | 1.42 | 1.39 | 1.31 | 1.52 | 0.85 | 0.79 | 0.78 | 0.81 |
| 10 | 1.40 | 1.46 | 1.46 | 1.45 | 0.82 | 0.87 | 0.87 | 0.86 |
| 12 | 1.49 | 1.48 | 1.52 | 1.47 | 0.88 | 0.86 | 0.92 | 0.95 |
| 14 | 1.54 | 1.50 | | 1.59 | 0.98 | 1.14 | | 0.96 |
| 16 | 1.60 | 1.64 | | | 0.95 | 1.00 | | 1.22 |
| 18 | 1.64 | 1.67 | | | | 1.05 | | |
| 20 | | 1.94 | | | | 1.21 | | |
| 22 | | 2.07 | | | | | | |

[a] The values of $\Gamma_0$ and $\alpha$ given for each band, with statistical uncertainties in brackets, result from fitting all of the linewidths $\Gamma$ of the band to the formula $\Gamma = \Gamma_0 + \alpha N'(N' + 1)$.

TABLE II. Comparison of present and previous linewidths (cm$^{-1}$, FWHM) for the (1,0)–(12,0) Schumann–Runge bands of $O_2$.

| $v'$ | Present[a] | NCK[b] | Australian group | | | | FH[c] | J[d] |
|---|---|---|---|---|---|---|---|---|
| | | (1988) | (1986)[e] | (1981)[f] | (1979)[g] | (1978)[h] | (1979) | (1976) |
| 1 | 0.93 ± 0.18 | 0.9 | 0.66 | | | | | 0.45 |
| 2 | 0.72 ± 0.04 | 0.6 | 0.39 | | 0.62 | | 0.24 | 0.27 |
| 3 | 1.78 ± 0.11 | 1.8 | 1.61 | | 1.2 | | 1.84 | 1.30 |
| 4 | 3.87 ± 0.27 | 3.6 | 2.99 | | 3.0 | | 4.18 | 2.93 |
| 5 | 2.13 ± 0.07 | 2.0 | 1.91 | | 1.9 | | 2.34 | 1.33 |
| 6 | 1.79 ± 0.21 | 1.8 | 1.38 | | 1.41 | 1.43 | 1.11 | 1.80 |
| 7 | 2.01 ± 0.10 | 1.9 | 1.87 | 1.62 | 1.47 | 1.63 | 1.70 | 1.90 |
| 8 | 1.92 ± 0.12 | 2.1 | 1.61 | 1.36 | 1.23 | 1.35 | 1.43 | 1.59 |
| 9 | 1.01 ± 0.16 | 1.2 | 0.67 | 0.67 | 0.56 | 0.67 | 0.76 | 0.89 |
| 10 | 1.09 ± 0.08 | 1.0 | 0.95 | 0.70 | 0.78 | 0.69 | 0.42 | 0.67 |
| 11 | 1.48 ± 0.18 | 1.4 | 1.18 | 0.94 | 0.98 | 0.98 | 1.27 | 1.30 |
| 12 | 0.88 ± 0.14 | 0.8 | 0.42 | 0.66 | 0.57 | 0.60 | 0.81 | 0.70 |

[a] Values obtained by averaging all data in Table I.
[b] Values obtained by fitting our cross sections measured at 300 K; from Table IV of Nicolet, Cieslik, and Kennes (Ref. 21).
[c] Values obtained by fitting Voigt profiles to absorption measurements with a 2.2 m spectrometer; from Table III of Frederick and Hudson (Ref. 28).
[d] Calculated values; from Table III of Julienne (Ref. 12).
[e] Values extrapolated to zero rotation; from Table IV of Lewis et al. (Ref. 22).
[f] Values from Table IV of Gies et al. (Ref. 23).
[g] Values from Table III of Lewis et al. (Ref. 24).
[h] Values from Table V of Lewis et al. (Ref. 25).

linewidths from Table II are plotted with other experimental and theoretical values in Fig. 2.

We have examined our results listed in Table I for possible evidence of the dependence of the predissociation linewidth on rotational quantum number $N'$. To this end, we have fitted the linewidths $\Gamma$ for each band in Table I to an equation of the form $\Gamma = \Gamma_0 + \alpha N'(N' + 1)$, in which $\Gamma_0$ is the rotationless width and $\alpha$ expresses the rotational dependence. The values found for $\Gamma_0$ and $\alpha$ are listed in Table I, and have been used to obtain the (parabolic) curves plotted in Figs. 3(a)–3(d).

From Figs. 3(a)–3(d) and from analogous figures (not shown) for the other bands, we have drawn the following conclusions. Changes of linewidth, if any, are slight relative to experimental scatter for $v' = 3, 4, 5,$ and 7 [see Fig. 3(a) for $v' = 5$ and Fig. 3(c) for $v' = 7$]; apparent increases in

linewidth with increasing $N'$ occur for $v' = 2, 6, 8, 9, 11,$ and 12 [see Fig. 3(b) for $v' = 6$]; and marginal decreases in linewidth with increasing $N'$ occur for $v' = 1$ and 10 [see Fig. 3(d) for $v' = 10$]. The above conclusions concerning the rotational dependence of the linewidth are, nonetheless, tentative because they could be factitious consequences of the present assumptions, made faute de mieux, that (a) the predissociation linewidths of the fine structure components of a given rotational line are equal, and (b) the line center positions of the unresolved or partially resolved components obtained from our spectroscopic constants are of sufficient accuracy.

Additional reservations apply to the apparent rotational dependence of the line widths of the (9,0), (11,0), and (12,0) bands. For these bands, the lines with high $N$ values
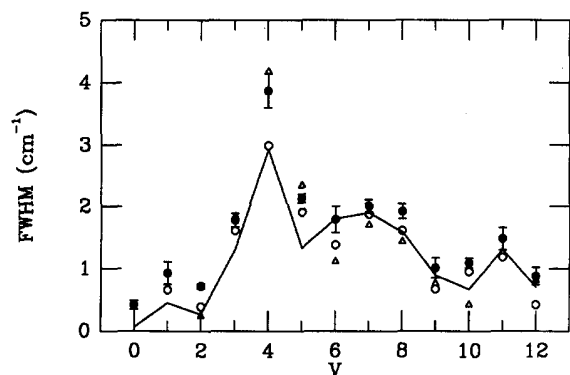


FIG. 2. Variation of the predissociation linewidth with vibrational quantum number in the $B\,^3\Sigma_u^-$ state of $O_2$. Filled circles—present average values; open circles—Lewis et al. (Ref. 22); triangles—Frederick and Hudson (Ref. 28). solid line—Juilenne (Ref. 12).
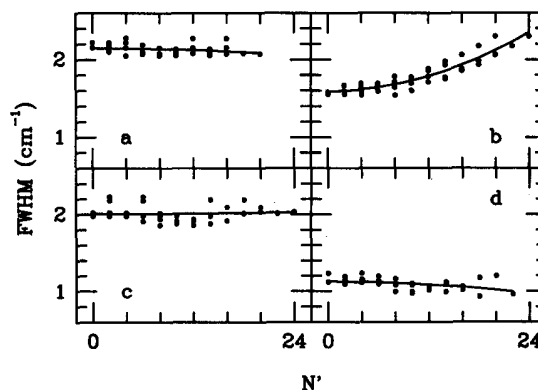


FIG. 3. The variation of the predissociation linewidth with upper rotational quantum number $N'$, shown in 3(a)–(d) for the $(v',0)$ Schumann–Runge bands of $O_2$ with $v' = 5, 6, 7,$ and 10. Discrete points—experimental predissociation widths from Table I; solid line—least-squares fit to $\Gamma = \Gamma_0 + \alpha N'(N' + 1)$ of experimental values $\Gamma$.
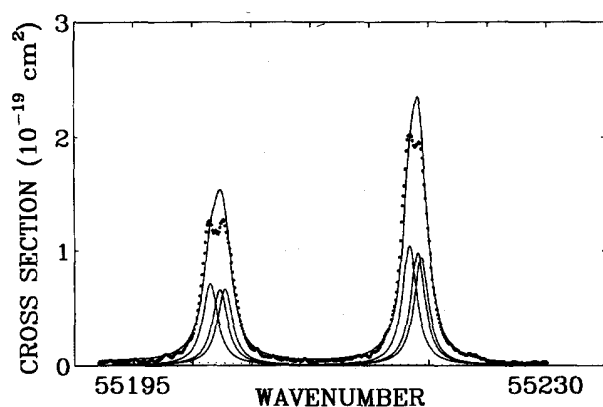
FIG. 4. Discrepancies in the fitting of experimental cross sections of some rotational features of the (11, 0) Schumann–Runge band of $O_2$ at 295 K. Uppermost curve synthesized from lower fine structure (Lorentzian) components to fit measured cross sections, represented by dots.

($N \geqslant 11$), unlike those of the (6,0) band, have not been fitted completely satisfactorily. Examples are the $P(15)$ and $R(17)$ lines of the (11,0) band shown in Fig. 4, and the $P(19)$ and $R(21)$ lines of the (9,0) band shown in Fig. 5. In each case, the experimental cross section shows structure near the line center that is not reproduced in the synthesized profile. This unsatisfactory aspect of the fitting worsens as $N$ increases, which suggests that the assumption (a) above, of equal linewidths for the fine structure components of a group, may be inadequate. Further work to achieve more realistic synthesized profiles for these bands is in progress. Wodtke et al.[19] have recently examined the excitation spectrum of a high rotational line $R(27)$ of the (11,2) band and found evidence for different linewidths for the triplet components. They ascribe their results to a $^3\Pi_u$ predissociative mechanism, a conclusion to which we have raised objections.[20] It is known theoretically[11,12] that the assumption of equal linewidths for the triplet components is approximately valid for a $^5\Pi_u$ predissociative mechanism, but not for $^3\Pi_u$ or $^3\Sigma_u^+$ mechanisms. Nonetheless, our results for low rotational lines of the (11,0) band[20] are consistent with, but do not necessarily require, an exclusively $^5\Pi_u$ mechanism.
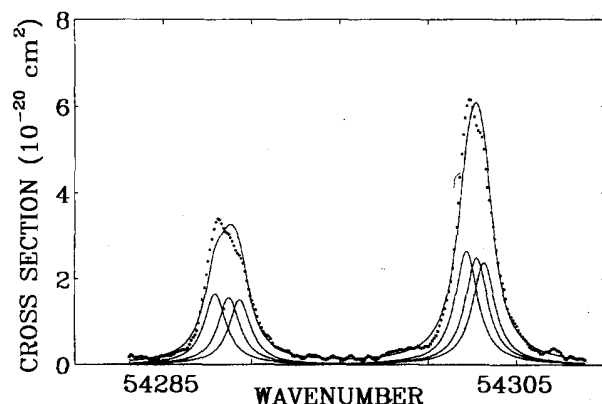


FIG. 5. The same as Fig. 4, except for the (9,0) band.

Comparison of our results for the predissociation linewidths with those of Nicolet et al.[21] is instructive because both are based on our experimental absolute absorption cross sections, but the modeling techniques used to extract the linewidths are rather different. To generate the absorption cross sections, Nicolet et al. employ band oscillator strengths based closely on our measured values.[6–8] With these adopted band oscillator strengths and Voigt line profiles, in which the Gaussian constituent has the calculated Doppler width and the Lorentzian constituent width defines the predissociation linewidth within a band, Nicolet et al. compute the absorption cross section and adjust the Lorentzian width to fit our measured absorption cross section of the band at room temperature. Their resultant predissociation linewidths are shown in Table II. Nicolet et al. tested those results derived from our cross section measurements at room temperature by comparing, in their Figs. 4–14, our cross section measurements at 79 K with their computed spectra, and the overall agreement is very satisfactory.

In our method of obtaining the predissociation linewidths, the individual fine structure components are represented by Lorentzian, not Voigt, profiles. An initial guessed linewidth is used to start an iterative procedure to procure a best least-squares fit between calculated and measured absorption cross sections. This technique is applied separately to our cross section measurements at 295 and 79 K (Table I). By fitting the measured cross sections directly, we avoid explicit use of our previously measured band oscillator strengths and, consequently, take into account implicitly any possible variation in band oscillator strength with temperature.

In Table I, consider, in connection with the possible temperature dependence of the linewidths, only those linewidths which, for any given $N'$, we have studied at both temperatures. For each of the bands (3,0)–(12,0), form separate average linewidth values corresponding to 79 and 295 K, and take the ratio of these averages. For these 10 bands, the mean of the ratios is found to be $1.00 \pm 0.03$. This result indicates that, within experimental uncertainty, the linewidths determined in our empirical Lorentzian formulation are independent of the temperature. The Doppler width, which is calculated to decrease by a factor of 1.93 from its value of $\sim 0.121$ cm$^{-1}$ at 295 K to $\sim 0.063$ cm$^{-1}$ at 79 K, is not included, a priori, in our purely Lorentzian model. The observed temperature independence of our empirical Lorentzian linewidths and the good agreement between our purely Lorentzian widths and the Lorentzian constituent linewidths of the Voigt profiles of Nicolet et al. indicate that, for the (1,0)–(12,0) bands, the assumption of Lorentzian profiles is adequate. In fact our Lorentzian linewidths in Table II exceed the Doppler widths by factors ranging from about 6 to 60.

The latest results of Lewis et al.[22] for the predissociation linewidths supersede the previous determinations of this Australian group,[23–25] as shown in Table II. In those determinations, band oscillator strengths and predissociation linewidths were adjusted simultaneously, in a detailed modeling scheme, to fit the equivalent widths of rotational features measured with a 2.2 or 6.65 m scanning monochroma-

tor. The systematic error arising from the inverse correlation between oscillator strength and linewidth in calculations of equivalent width should be minimal in their most recent study,[22] because their mean band oscillator strengths[26] are in good agreement with our direct, model-independent values from measurements of the integrated absolute cross sections.[6,7] Lewis *et al.*[22] did, however, use spectroscopic constants[26] differing slightly from ours[16] to calculate the line center positions of the fine structure components. The rotationless linewidths of Lewis *et al.*[22] in our Table II are all lower than our $\Gamma_0$ values in Table I by factors ranging from 1.07 for the (7,0) band to 2.10 for the (12,0) band; for $v' = 3, 5, 6, 7, 8$, and 11, these systematic differences in rotationless linewidths are relatively small, but for $v' = 1, 2, 4, 9,$ 10, and 12, the systematic differences are unacceptably large. In this context, the good agreement between the linewidths of Lewis *et al.*[22] and our previously published linewidths near the bandheads of the (14,0), (15,0), and (16,0) bands[27] is perhaps surprising, because those linewidths are smaller (0.18–0.40 cm$^{-1}$) and our determination involved matching our observed, instrumentally degraded (i.e., not absolute) cross sections with an artificially degraded, synthesized cross section by varying both the oscillator strength and linewidth in the computed spectrum of Voigt profiles. In spite of these quantitative disagreements on the linewidths of the bands with $v' = 1$–12, Fig. 2 illustrates the similarity in overall patterns of the widths which show maxima at $v' = 4, 7,$ and 11, and minima at $v' = 6, 9,$ and 12. The maxima in the earlier experimental values of Frederick and Hudson[28] and in the calculated values of Julienne[12] also occur at $v' = 4, 7,$ and 11.

The linewidths represented by the solid line in Fig. 2 are those calculated by Julienne[12] from contributions made to the predissociation by four repulsive states, viz., $^3\Sigma_u^+$, $^1\Pi_u$, $^3\Pi_u$, and $^5\Pi_u$. Lewis *et al.*[22] have adjusted the model parameters of Julienne[12] to fit their own experimental linewidths better, but their adjusted value of the spin–orbit coupling strength for the $^5\Pi_u$ state does not result in a smooth deperturbation of second vibrational differences for all three isotopic species $^{16}O_2$, $^{16}O^{18}O$, and $^{18}O_2$ for the vibrational levels considered to be most affected by the $^5\Pi_u$ state.[29] The conclusion of Julienne,[12] that the $^5\Pi_u$ state is primarily, though not exclusively, responsible for the predissociation in most of the levels $3 < v' < 12$, is supported by our study of the isotopic shifts.[29] The ratio of the fine structure component linewidths calculated by Julienne[12] for a $^5\Pi_u$ predissociative mechanism is close to the ratio 1:1:1 for the $F_1$, $F_2$, and $F_3$ components, which corresponds to our assumption (a) above.

In view of the limitations existing at present in our and in previous determinations of the linewidths, and because we hope in the future to investigate some of the constraints responsible, only a brief comparison is now made with the study by Lewis *et al.*[22] of the rotational dependence. They find increases in linewidths with increasing rotation for $v' = 6, 8, 9,$ and 12, as we do, and also for $v' = 3$, where we find no marked trend. They find decreases in linewidths with increasing rotation for $v' = 5, 7, 10,$ and 11, whereas we find no clear trend for $v' = 5$ and 7, a marginal decrease for

$v' = 10$, and an increase for $v' = 11$.

A recent linewidth study, of only the (5, 0) band, by a totally different technique involving Raman excitation profiles has yielded a linewidth, 2.05 cm$^{-1}$, which is almost independent of the rotational quantum number.[30] This determination is in good accord with our average value of 2.13 cm$^{-1}$ (Table II) and with the rotational dependence (or, rather, the lack of it) shown in our Fig. 3(a). In contrast, Lewis *et al.*[22] find an extrapolated rotationless value of 1.91 cm$^{-1}$, which decreases with increasing rotational quantum number.

The highest pressures used in our absorption cross section measurements, at 295 and 79 K, from which our present linewidths in Table I are derived, were $\sim 300$ and 150 Torr, respectively, and the use of 300 Torr at 295 K was for the weak (1,0) and (2,0) bands. According to the pressure broadening measurements of Lewis *et al.*,[31] the self-broadening coefficient is 0.20 cm$^{-1}$ (FWHM) atm$^{-1}$, so that the contribution to our linewidths would be less than $\sim 0.08$ cm$^{-1}$ for the (1,0) and (2,0) bands and still less for the other bands. Zhang and Ziegler[30] have found that the predissociation linewidth of the (5,0) band is independent of oxygen pressure in the range 0.5–2 atm. We are, therefore, disinclined to try to adjust our linewidths in Tables I and II for the effects, if any, of pressure.

The absorption cross section of the feeble (0,0) band with $P(N)$ and $R(N)$ lines with $3 < N < 11$ has also been analyzed. The experimental FWHM of the unresolved structures is $\sim 1$ cm$^{-1}$ and the individual linewidth obtained tentatively from our analysis is $0.47 \pm 0.07$ cm$^{-1}$. Let us assume that our cross section measurements of the (0, 0) band[8] are absolute, but may be subject to pressure broadening at the pressures (up to 1 atm) used for this weak band. The agreement between our measured band oscillator strength $2.59 \times 10^{-10}$, and our calculated value[32] $2.47 \times 10^{-10}$ supports this view because the band oscillator strength is not expected to be affected much by pressure broadening. The quadratic sum of a rough estimate ($\sim 0.2$ cm$^{-1}$) of the pressure-broadened width and the Doppler width (0.12 cm$^{-1}$) is $\sim 0.23$ cm$^{-1}$. Thus, a predissociation width considerably larger than the value 0.06 cm$^{-1}$ calculated by Julienne would be required to reach the value $0.47 \pm 0.07$ cm$^{-1}$ from our Lorentzian analysis, which may be inappropriate for the (0,0) band due to deviations from the Lorentzian shape that we observe near the wings.

## IV. CONCLUDING REMARKS

Predissociation linewidth determinations presented here for the (1,0) to (12,0) Schumann–Runge bands of oxygen are independent of instrumental width and are believed to be the most accurate currently available. The best available molecular constants were used to calculate the line center positions of fine structure components and the measured absorption cross sections were fitted directly. Rotational dependence of predissociation linewidths has been examined and is most marked for bands with $v' = 6, 9, 11,$ and 12. Further work to improve the fitting of the (9,0), (11,0), and (12,0) experimental cross sections by using different predis-

sociation widths for the fine structure components of a rotational line is in progress.

Many of the linewidths deduced in the present work differ significantly from those of earlier studies, so that reexamination of calculations of solar flux penetration into the Earth's atmosphere and photodissociation rates of some trace species may be warranted, as has been discussed by Nicolet and Kennes.[3]

## ACKNOWLEDGMENTS

[1] J. E. Frederick and R. D. Hudson, J. Atm. Sci. **31**, 1888 (1980).

[2] K. Omidvar and J. E. Frederick, Planet. Space Sci. **35**, 769 (1987).

[3] M. Nicolet and R. Kennes, Planet. Space Sci. **36**, 1059 (1988).

[4] R. D. Hudson, Rev. Geophys. Space Phys. **9**, 305 (1971).

[5] M. Ackerman, F. Biaumé, and G. Kockarts, Planet. Space Sci. **18**, 1639 (1970).

[6] K. Yoshino, D. E. Freeman, J. R. Esmond, and W. H. Parkinson, Planet. Space Sci. **31**, 339 (1983).

[7] K. Yoshino, D. E. Freeman, J. R. Esmond, and W. H. Parkinson, Planet. Space Sci. **35**, 1067 (1987).

[8] A. S-C. Cheung, K. Yoshino, W. H. Parkinson, and D. E. Freeman, Can. J. Phys. **62**, 1752 (1984).

[9] K. Yoshino, D. E. Freeman, and W. H. Parkinson, Appl. Opt. **19**, 66 (1980).

[10] P. G. Wilkinson and R. S. Mulliken, Astrophys. J. **125**, 594 (1957).

[11] P. S. Julienne and M. Krauss, J. Mol. Spectrosc. **56**, 270 (1975).

[12] P. S. Julienne, J. Mol. Spectrosc. **63**, 60 (1976).

[13] C. S. Fadley, Ph.D. thesis, University of California, Berkeley (1970).

[14] Y. S. Chang and J. H. Shaw, Appl. Spectrosc. **31**, 213 (1977).

[15] M. A. Smith, C. P. Rinsland, B. Fridovich, and K. N. Rao, in *Intensities and collision broadening parameters from infrared spectra in Molecular Spectroscopy: Modern Research*, edited by K. N. Rao (Academic, New York, 1985), Vol. 3.

[16] A. S.-C. Cheung, K. Yoshino, W. H. Parkinson, and D. E. Freeman, J. Mol. Spectrosc. **119**, 1 (1986).

[17] J. B. Tatum and J. G. K. Watson, Can. J. Phys. **49**, 2693 (1971).

[18] P. Minguzzi and A. DiLieto, J. Mol. Spectrosc. **109**, 388 (1985).

[19] A. M. Wodtke, L. Hüwel, H. Schüter, H. Voges, G. Meyer, and P. Andresen, J. Chem. Phys. **89**, 1929 (1988).

[20] D. E. Freeman, A. S.-C. Cheung, K. Yoshino, and W. H. Parkinson, J. Chem. Phys. **91**, 6538 (1989).

[21] M. Nicolet, S. Cieslik, and R. Kennes, Planet. Space Sci. **36**, 1039 (1988).

[22] B. R. Lewis, L. Berzins, J. H. Carver, and S. T. Gibson, J. Quant. Spectrosc. Radiat. Transfer. **36**, 187 (1986).

[23] H. P. F. Gies, S. T. Gibson, D. G. McCoy, A. J. Blake, and B. R. Lewis, J. Quant. Spectrosc. Radiat. Transfer. **26**, 469 (1981).

[24] B. R. Lewis, J. H. Carver, T. I. Hobbs, D. G. McCoy, and H. P. F. Gies, J. Quant. Spectrosc. Radiat. Transfer. **22**, 213 (1979).

[25] B. R. Lewis, J. H. Carver, T. I. Hobbs, D. G. McCoy, and H. P. F. Gies, J. Quant. Spectrosc. Radiat. Transfer. **20**, 191 (1978).

[26] B. R. Lewis, L. Berzins, and J. H. Carver, J. Quantum. Spectrosc. Radiat. Transfer **36**, 209 (1986).

[27] P. L. Smith, H. E. Griesinger, J. H. Black, K. Yoshino, and D. E. Freeman, Astrophys. J. **277**, 569 (1984).

[28] J. E. Frederick and R. D. Hudson, J. Mol. Spectrosc. **74**, 247 (1979).

[29] A. S-C. Cheung, K. Yoshino, D. E. Freeman, R. S. Friedman, A. Dalgarno, and W. H. Parkinson, J. Mol. Spectrosc. **134**, 362 (1989).

[30] Y. P. Zhang and L. D. Ziegler, J. Phys. Chem. **93**, 6665 (1989).

[31] B. R. Lewis, L. Berzins, C. D. Dedman, T. T. Scholz, and J. H. Carver, J. Quantum. Spectrosc. Radiat. Transfer **39**, 271 (1988).

[32] K. Yoshino, D. E. Freeman, J. R. Esmond, R. S. Friedman, and W. H. Parkinson, Planet. Space Sci. **36**, 1201 (1988).